

MZ-TH/03-10

hep-ph/0307290

July 2003

Lectures on configuration space methods for sunrise-type diagrams

Stefan Groote

Institut für Physik der Johannes-Gutenberg-Universität,
Staudinger Weg 7, 55099 Mainz, Germany

Calc2003, Dubna, June 16–18th, 2003

Abstract

In this lecture series I will give a fundamental insight into configuration space techniques which are of help to calculate a broad class of Feynman diagrams, the sunrise-type diagrams. Applications are shown along with basic concepts and techniques.

Contents

1	Introduction	3
2	Concepts of configuration space techniques	4
2.1	The correlator function in momentum space	5
2.2	The renormalization	7
2.3	The momentum subtraction	8
2.4	A second example	9
2.5	A third example	11
2.6	The spectral density	12

3	Recurrence relations and transcendental numbers	13
3.1	The example $B_N(0, 0, 2, 2, 2, 2)$	13
3.2	The example $B_N(0, 0, 2, 2, 2, 1)$	15
3.3	The example $B_N(0, 0, 2, 3, 3, 4)$	15
3.4	The reduction procedure	16
3.5	The efficiency of the reduction	18
3.6	Values for the master integrals	18
3.7	Back to the genuine sunset	20
3.8	Generalization to the spectacle topology	21
4	Expansions close to threshold	23
4.1	Considerations in Minkowskian domain	24
4.2	Large x behaviour of the weight	24
4.3	The polarization function $\tilde{\Pi}^+(p)$	25
4.4	The polarization function $\tilde{\Pi}^-(p)$	26
4.5	Comment on the regularization used	27
4.6	The difference part $\tilde{\Pi}^{di}(p)$	28
4.7	The asymptotic part $\tilde{\Pi}^{as}(p)$	28
4.8	First example: equal mass ($n = 3$) sunrise diagram	29
4.9	Second example: equal mass $n = 4$ sunrise-type diagram	31
4.10	Strongly asymmetric mass arrangement	32
4.11	A last diagram	34

1 Introduction

There has been a renewal of interest in calculating the loop integral of a simple topology, the so-called generalized sunrise (or sunset, water melon, banana, basketball) diagrams [1, 2, 3, 4, 5]. The two-loop sunrise diagrams with different values of internal masses have been recently studied in some detail (see e.g. [6, 7, 8, 9, 10, 11] and references therein). In this lecture series I outline the configuration space technique [12, 13, 14, 15, 16, 17, 18, 19]. It can be used to verify the results obtained within other techniques [20, 21, 22, 23] and to investigate some general questions of Feynman diagram calculation [4, 15, 24, 25, 26, 27, 28, 29, 30]. The diagram with the sunrise topology form a subset of the general set of diagram with a given number of loops [31]. They appear in various specific physics applications:

- sum rules for baryonic currents [32, 33, 34, 35, 36, 37, 38, 39]
- gluonic correlators [40, 41, 42]
- multiloop calculations [43, 1]
- decays with multi-particle phase-space [44]
- lattice QCD calculations [45]
- mixing of neutral mesons [46]
- Chiral perturbation theory (ChPT) and effective theories for Goldstone modes in higher orders of momentum expansion [47, 7, 11]
- exotics [48, 49]
- effective potentials for symmetry breaking [50, 51]
- finite temperature calculations [54, 51, 53, 9, 52, 56, 55]
- applications in nuclear physics [57]
- applications in solid state physics [58]

2 Concepts of configuration space techniques

I will start this lecture series with explaining the basic elements that occur in calculating sunrise-type diagrams. The genuine sunrise diagram with three internal lines is shown on the left hand side in Fig. 1. It is the leading order perturbative correction to the lowest order propagator in ϕ^4 -theory. The corresponding leading order perturbative correction in ϕ^3 -theory is a one-loop diagram and can be considered as a degenerate case of the prior example. A straightforward generalization of this topology is a correction to the free propagator in ϕ^{n+1} -theory that contains $(n - 1)$ loops and n internal lines (see the right hand side of Fig. 1).

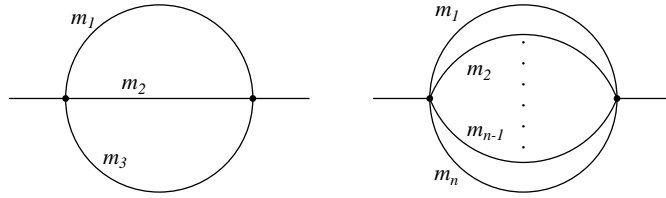


Figure 1: Genuine sunrise and general topology of the class of sunrise-type diagrams

In configuration space, the “calculation” of the correlator two-point function is very easy. It is just given by the product of the propagators,

$$\Pi(x) = \prod_i D(x, m_i). \quad (1)$$

The propagators themselves (for the scalar case and massive particles) are solutions of the Klein–Gordon equation and can be written in D -dimensional Euclidean space-time as

$$D(x, m) = \int \frac{d^D p}{(2\pi)^D} \frac{e^{ip_\mu x^\mu}}{p^2 + m^2} = \frac{(mx)^\lambda K_\lambda(mx)}{(2\pi)^{\lambda+1} x^{2\lambda}} = \frac{(m/x)^\lambda}{(2\pi)^{\lambda+1}} K_\lambda(mx) \quad (2)$$

where I used $D = 2\lambda + 2$ for convenience, $x = \sqrt{x_\mu x^\mu}$, and $K_\lambda(z)$ is the modified Bessel function of the second kind (see e.g. [59]). Frankly speaking, the propagator $D(x, m)$ describes the propagation of a particle of mass m from the space-time point 0 to x (a situation which of course is invariant with respect to translation). For $m = 0$ we obtain

the massless propagator

$$D(x, 0) = \int \frac{d^D p}{(2\pi)^D} \frac{e^{ik_\mu x^\mu}}{p^2} = \frac{\Gamma(\lambda)}{4\pi^{\lambda+1} x^{2\lambda}} \quad (3)$$

simply by calculating the limit, taking into account the series expansion of the Bessel function $K_\lambda(mx)$ which will be shown later on. Modified internal lines can also occur, as a result of a reduction procedure of more complicated diagrams or as diagrams with mass insertion on a line. These insertions are indicated by one or more dots placed on the line. Again, the representation of these cases is easily established,

$$D^{(\mu)}(x, m) = \int \frac{d^D p}{(2\pi)^D} \frac{e^{ip_\mu x^\mu}}{(p^2 + m^2)^{\mu+1}} = \frac{(m/x)^{\lambda-\mu}}{(2\pi)^{\lambda+1} 2^\mu \Gamma(\mu+1)} K_{\lambda-\mu}(mx) \quad (4)$$

(note that $D^{(\mu)}(x, m)$ is related to the μ -th derivative with respect to the parameter m^2). It is obvious that, up to different power in x and normalization, a modification of the internal line just changes the index of the Bessel function. The modified propagator has the same functional form as the usual propagator. This matter of fact unifies and simplifies the considerations.

The generalization to more complicated integrands with additional tensor structure $p^{\mu_1} \dots p^{\mu_k}$ is straightforward as well. Because of

$$\int \frac{d^D p}{(2\pi)^D} \frac{p_\nu e^{ip_\mu x^\mu}}{p^2 + m^2} = -i \frac{\partial}{\partial x^\nu} \int \frac{d^D p}{(2\pi)^D} \frac{e^{ip_\mu x^\mu}}{p^2 + m^2} = -i \frac{x_\nu}{x} \frac{\partial}{\partial x} \left(\frac{(mx)^\lambda K_\lambda(mx)}{(2\pi)^{\lambda+1} x^{2\lambda}} \right), \quad (5)$$

this merely leads again to different orders of the Bessel function, together with a tensor structure $x^{\mu_1} \dots x^{\mu_k}$. However, these tensor structure does not matter in taking simply the product of the propagators. We can conclude that in order to obtain the expression for the correlator function in configuration space there is no integration at all.

2.1 The correlator function in momentum space

An integration occurs, if we want to calculate the correlator function in momentum space, being the Fourier transform of $\Pi(x)$,

$$\tilde{\Pi}(p) = \int \Pi(x) e^{ip_\mu x^\mu} d^D x. \quad (6)$$

For a general tensor structure, the integral is calculated by expanding the plane wave function $\exp(ip_\mu x^\mu)$ in a series of Gegenbauer polynomials $C_j^\lambda(p_\mu x^\mu/px)$. The Gegenbauer polynomials are a generalizations of associated Legendre polynomials to the D -dimensional space-time. They are determined by the characteristic polynomial

$$(t^2 - 2tz + 1)^{-\lambda} = \sum_{l=0}^{\infty} t^l C_l^\lambda(z) \quad (7)$$

and are given by $C_0^\lambda(z) = 1$, $C_1^\lambda(z) = 2\lambda z$ and the recursion formula

$$(l+1)C_{l+1}^\lambda(z) = 2(l+\lambda)zC_l^\lambda(z) - (l+2\lambda-1)C_{l-1}^\lambda(z) = 0. \quad (8)$$

The Gegenbauer polynomials satisfy the orthogonality relations ($\hat{x}_i = x_i/|x_i|$)

$$\int C_m^\lambda(\hat{x}_1 \cdot \hat{x}_2) C_n^\lambda(\hat{x}_2 \cdot \hat{x}_3) d^D \hat{x}_2 = \frac{2\pi^{\lambda+1}}{\Gamma(\lambda+1)} \frac{\lambda \delta_{mn}}{\lambda+n} C_n^\lambda(\hat{x}_1 \cdot \hat{x}_3) \quad (9)$$

on the D -dimensional unit sphere with rotationally invariant measure $d^D \hat{x}_2$ where

$$\int d^D \hat{x}_2 = \frac{2\pi^{\lambda+1}}{\Gamma(\lambda+1)}. \quad (10)$$

Expressed in terms of Gegenbauer polynomials, the plane wave reads

$$\exp(ip_\mu x^\mu) = \Gamma(\lambda) \left(\frac{px}{2}\right)^{-\lambda} \sum_{l=0}^{\infty} i^l (\lambda+l) J_{j+l}(px) C_l^\lambda(p_\mu x^\mu / px) \quad (11)$$

where $J_\lambda(z)$ is the Bessel function of the first kind and $p = \sqrt{p_\mu p^\mu}$. This formula allows one to single out an irreducible tensorial structure from the angular integration in the Fourier integral. Integration techniques involving Gegenbauer polynomials for the computation of massless diagrams are described in Detail in [60] where many useful relations can be found (see also [61]). In case of absence of explicit tensorial structure, however, the orthogonality relations for Gegenbauer polynomials can be used to explicitly integrate over the unit sphere,

$$\int e^{ip_\mu x^\mu} d^D \hat{x} = 2\pi^{\lambda+1} \left(\frac{px}{2}\right)^\lambda J_\lambda(px). \quad (12)$$

In the following I will concentrate on this scalar case. The Fourier transform of the sunrise-type diagram, therefore, is given by the one-dimensional integral

$$\tilde{\Pi}(p) = 2\pi^{\lambda+1} \int_0^\infty \left(\frac{px}{2}\right)^{-\lambda} J_\lambda(px) D(x, m_1) \cdots D(x, m_n) x^{2\lambda+1} dx. \quad (13)$$

2.2 The renormalization

While the configuration space expression for the sunrise-type diagram contains no integration, it does not always represent an integrable function for a generic value of space-time dimension D . $\Pi(x)$ can have non-integrable singularities at small x for a sufficiently large number of propagators when $D > 2$ [62]. The reason is that each propagator by itself can be considered as a distribution. However, distributions do not form an algebra and multiplication is not well-defined. In this respect the correlator function $\Pi(x)$ is not completely defined as a proper distribution. In attempting to integrate such a function over the whole x -space we encounter infinities which are usual UV divergencies. Therefore, the computation of its Fourier transform requires regularization (for instance, dimensional regularization) and subtraction.

UV divergencies given as poles in ε for the dimensional regularization are related to short distances x . Therefore, one should expand massive propagators at small x to obtain the counterterms. Still a convergence at large x should be retained which provides IR regularization (see e.g. [63]). This technical constraint can be met for instance by keeping one (or two) massive propagators unexpanded. The possibility is given because the integrals of one or two Bessel functions are known [64, 65].

However, one can do even simpler by using a damping function like $e^{-\mu^2 x^2}$ to suppress contributions for large values of x , corresponding to IR singularities. This is done by introducing the factor $1 = e^{\mu^2 x^2} e^{-\mu^2 x^2}$ into the integrand. In this case all massive propagators along with the factor $e^{\mu^2 x^2}$ can be expanded in small values of x . The expansion of the propagators is straightforward and results from the definitions

$$J_\lambda(z) = \left(\frac{z}{2}\right)^\lambda \sum_{k=0}^{\infty} \frac{(-z^2/4)^k}{k! \Gamma(\lambda + k + 1)} = \frac{(z/2)^\lambda}{\Gamma(1 + \lambda)} \left(1 - \frac{(z/2)^2}{1 + \lambda} + \dots\right) \quad (14)$$

and

$$K_\lambda(z) = \frac{\pi}{2} \frac{I_{-\lambda}(z) - I_\lambda(z)}{\sin(\pi\lambda)}, \quad \Gamma(\lambda)\Gamma(1 - \lambda) = \frac{\pi}{\sin(\pi\lambda)} \quad (15)$$

with

$$I_\lambda(z) = \left(\frac{z}{2}\right)^\lambda \sum_{k=0}^{\infty} \frac{(z^2/4)^k}{k! \Gamma(\lambda + k + 1)} \quad (16)$$

Therefore, one has

$$\left(\frac{z}{2}\right)^\lambda K_\lambda(z) = \frac{\Gamma(\lambda)}{2} \left[1 + \frac{1}{1-\lambda} \left(\frac{z}{2}\right)^2 - \frac{\Gamma(1-\lambda)}{\Gamma(1+\lambda)} \left(\frac{z}{2}\right)^{2\lambda} \right] + O(z^4, z^{2+2\lambda}). \quad (17)$$

The final integration can be done formally by using the identity

$$\int_0^\infty x^{r-1} e^{-\mu^2 x^2} dx = \frac{1}{2} \mu^{-r} \Gamma(r/2). \quad (18)$$

As an example we consider the genuin sunrise diagram with three different masses m_1 , m_2 , and m_3 , given in configuration space by

$$\Pi(x) = D(x, m_1) D(x, m_2) D(x, m_3). \quad (19)$$

The counterterms for the Fourier transform

$$\tilde{\Pi}(p) = 2\pi^{\lambda+1} \int_0^\infty \left(\frac{px}{2}\right)^{-\lambda} J_\lambda(px) D(x, m_1) D(x, m_2) D(x, m_3) x^{2\lambda+1} dx \quad (20)$$

are obtained by introducing $e^{\mu^2 x^2} e^{-\mu^2 x^2}$ and expanding the occuring Bessel functions as well as $e^{\mu^2 x^2}$. The singular parts we obtain for dimensional regularization with $D = 4 - 2\varepsilon$, i.e. $\lambda = 1 - \varepsilon$, are given by

$$\tilde{\Pi}_{\text{sing}}(p) = \frac{\mu^{-4\varepsilon}}{\pi^{4-2\varepsilon}} \left\{ -\frac{m_1^2 + m_2^2 + m_3^2}{512\varepsilon^2} + \frac{1}{\varepsilon} \left(\sum_{i=1}^3 \frac{m_i^2 \ln(m_i e^{\gamma'}/2\mu)}{128} - \frac{p^2}{1024} \right) \right\} \quad (21)$$

where $\gamma' = \gamma_E/2 - 3/4$. Note, though, that the result is given in Euclidean domain. In this way one easily finds pole parts for any diagram with any mass arrangement.

2.3 The momentum subtraction

Renormalization by momentum subtraction is the oldest renormalization method. The idea is to subtract the integrand in some specific momentum point. For massive diagrams the point $p = 0$ is IR-safe, and the receipe is realized for instance by expanding the function

$$\left(\frac{px}{2}\right)^{-\lambda} J_\lambda(px) \quad (22)$$

which is the kernel or weight function of the integral transformation) in a Taylor series around $p = 0$ in terms of a polynomial series in p^2 . The subtraction of order N is achieved by writing

$$\left[\left(\frac{px}{2} \right)^{-\lambda} J_\lambda(px) \right]_N = \left(\frac{px}{2} \right)^{-\lambda} J_\lambda(px) - \sum_{k=0}^N \frac{(-1)^k}{k! \Gamma(\lambda + k + 1)} \left(\frac{px}{2} \right)^{2k} \quad (23)$$

and by keeping N terms in the expansion on the right hand side. The number N of necessary subtractions is determined by the divergence index of the diagram and can be found according to the standard rules of the R -operation [62]. For the example we started with, a momentum subtraction which is symmetric in the masses m_1 , m_2 , and m_3 leads to the finite part

$$\tilde{\Pi}_{\text{fin}}(p) = 2\pi^{\lambda+1} \int_0^\infty \left[\left(\frac{px}{2} \right)^{-\lambda} J_\lambda(px) \right]_N D(x, m_1) D(x, m_2) D(x, m_3) x^{2\lambda+1} e^{\mu^2 x^2} e^{-\mu^2 x^2} dx \quad (24)$$

where N is the order of expansion which has to be chosen for integrability. This is of course the same order which has been used earlier in order to extract the counterterms. It is obvious, though, that the expansion can cease at positive powers of x . Finally, $\varepsilon = 0$ can be taken to calculate the finite part. As a technical remark note that most numerical integration routines will run into problems if the upper limit is kept to be infinity. However, already for values of the order $x \sim 1$ the integrand is negligible, so that the integration can terminate at this point. Also the region about the origin might cause trouble. In this case the integration interval can be subdivided close to the origin, and the whole integrand for the subinterval to zero can be expanded in x as a whole. For specific values of p^2 , m_1 , m_2 , and m_3 we could reproduce results given in the literature (e.g. results given in [21, 66]).

2.4 A second example

The second example I want to show here starts with the same genuine sunrise diagram but is evaluated for a special setting of the masses. The reason is that there exists an analytical expression in the literature [10]. In this example the subtraction is done in several steps. The first step consists of a momentum subtraction for the weight function with $N = 1$.

We obtain

$$\tilde{\Pi}(p) = \tilde{\Pi}_{\text{mom}}(p) + \tilde{\Pi}_{\text{rem}}(p) \quad \text{where} \quad (25)$$

$$\begin{aligned} \tilde{\Pi}_{\text{mom}}(p) &= 2\pi^{\lambda+1} \int_0^\infty \left[\left(\frac{px}{2} \right)^{-\lambda} J_\lambda(px) \right]_1 D(x, m_1) D(x, m_2) D(x, m_3) x^{2\lambda+1} dx = \\ &= 2\pi^{\lambda+1} \int_0^\infty \left[\left(\frac{px}{2} \right)^{-\lambda} J_\lambda(px) - \frac{1}{\Gamma(\lambda+1)} + \frac{p^2 x^2}{4} \frac{1}{\Gamma(\lambda+2)} \right] \times \\ &\quad \times D(x, m_1) D(x, m_2) D(x, m_3) x^{2\lambda+1} dx, \end{aligned} \quad (26)$$

$$\begin{aligned} \tilde{\Pi}_{\text{rem}}(p) &= A + p^2 B = \\ &= \frac{2\pi^{\lambda+1}}{\Gamma(\lambda+1)} \int_0^\infty D(x, m_1) D(x, m_2) D(x, m_3) x^{2\lambda+1} dx + \\ &\quad - p^2 \frac{2\pi^{\lambda+1}}{4\Gamma(\lambda+2)} \int_0^\infty x^2 D(x, m_1) D(x, m_2) D(x, m_3) x^{2\lambda+1} dx. \end{aligned} \quad (27)$$

The analytical result in [10] is given at the pseudothreshold $p = m_1 + m_2 - m_3$. For simplicity we choose $m_1 = m_2 = m_3/2 = m$. In this case we obtain $p = 0$, $\tilde{\Pi}_{\text{mom}}(0) = 0$ and the vanishing of the counterterm $p^2 B$. Only

$$A = \frac{2\pi^{\lambda+1}}{\Gamma(\lambda+1)} \int_0^\infty D(x, m) D(x, m) D(x, 2m) x^{2\lambda+1} dx \quad (28)$$

has to be determined. In order to separate singular and finite part as $(2\pi)^D A = S + F$ (where the total normalization of [10] has been adopted) we use momentum subtraction for the last Bessel function $K_\lambda(2mx)$ and obtain for the singular part

$$\begin{aligned} S &= \frac{(2\pi)^D m^{2\lambda}}{\Gamma(\lambda+1)} \int_0^\infty x^{1-2\lambda} K_\lambda(mx) K_\lambda(mx) \frac{\Gamma(\lambda)}{2} \left[1 + \frac{(mx)^2}{1-\lambda} - \frac{\Gamma(1-\lambda)}{\Gamma(1+\lambda)} (mx)^{2\lambda} \right] dx = \\ &= \pi^{4-2\varepsilon} \frac{m^{2-4\varepsilon} \Gamma^2(1+\varepsilon)}{(1-\varepsilon)(1-2\varepsilon)} \left[-\frac{3}{\varepsilon^2} + \frac{8 \ln 2}{\varepsilon} + 8(2 - 2 \ln 2 - \ln^2 2) \right] + O(\varepsilon) \end{aligned} \quad (29)$$

where we could make use of

$$\int_0^\infty x^{2\alpha-1} K_\mu(mx) K_\mu(mx) dx = \frac{2^{2\alpha-3}}{m^{2\alpha} \Gamma(2\alpha)} \Gamma(\alpha+\mu) \Gamma(\alpha) \Gamma(\alpha) \Gamma(\alpha-\mu). \quad (30)$$

In comparing the part S with the analytical result in [10] for $p = 0$,

$$\tilde{\Pi}_{\text{ref}}(0) = \pi^{4-2\varepsilon} \frac{m^{2-4\varepsilon} \Gamma^2(1+\varepsilon)}{(1-\varepsilon)(1-2\varepsilon)} \left[-\frac{3}{\varepsilon^2} + \frac{8 \ln 2}{\varepsilon} - 8 \ln^2 2 \right] + O(\varepsilon), \quad (31)$$

one obtains the same singular parts while the difference of the finite parts is expected to be found in the part F . Indeed, one obtains

$$F = \frac{(2\pi)^D m^{2\lambda}}{\Gamma(\lambda+1)} \int_0^\infty x^{2(1-\lambda)-1} K_\lambda(mx) K_\lambda(mx) \times \\ \times \left\{ (mx)^\lambda K_\lambda(2mx) - \frac{\Gamma(\lambda)}{2} \left[1 + \frac{(mx)^2}{1-\lambda} - \frac{\Gamma(1-\lambda)}{\Gamma(1+\lambda)} (mx)^{2\lambda} \right] \right\} dx \quad (32)$$

which is finite and can therefore be calculated for $D = 4$,

$$F = 16\pi^4 m^2 \int_0^\infty \frac{dx}{x} K_1(x) K_1(x) \left\{ x K_1(2x) - \frac{1}{2} [1 + x^2(-1 + 2\gamma_E + 2 \ln x)] \right\}. \quad (33)$$

It is shown numerically that $F = 16\pi^4 m^2 (\ln 2 - 1)$, and because this quantity is finite, the normalization can be restored, we obtain

$$F = \pi^{4-2\varepsilon} \frac{m^{2-4\varepsilon} \Gamma^2(1+\varepsilon)}{(1-\varepsilon)(1-2\varepsilon)} 16(\ln 2 - 1) + O(\varepsilon). \quad (34)$$

2.5 A third example

An example for the three-loop case is the sunrise-type diagram with two massive and two massless lines at vanishing external momentum. The analytical expression for the diagram in configuration space representation is given by

$$\tilde{\Pi}(0) = \int (D(x, m))^2 (D(x, 0))^2 d^D x = \int \left(\frac{(mx)^\lambda K_\lambda(mx)}{(2\pi)^{\lambda+1} x^{2\lambda}} \right)^2 \left(\frac{\Gamma(\lambda)}{4\pi^{\lambda+1} x^{2\lambda}} \right)^2 d^D x. \quad (35)$$

While the angular integration in D -dimensional space-time is trivial,

$$\int e^{ip_\mu x^\mu} d^D \hat{x} = 2\pi^{\lambda+1} \left(\frac{px}{2} \right)^{-\lambda} J_\lambda(px) \rightarrow \frac{2\pi^{\lambda+1}}{\Gamma(\lambda+1)} \quad \text{for } p \rightarrow 0, \quad (36)$$

the problem of residual radial integration is solved by Eq. (30). The result reads

$$\tilde{\Pi}(0) = \left(\frac{m^2}{4} \right)^{3\lambda-1} \frac{1}{2^8 \pi^{3\lambda+3}} \frac{\Gamma(\lambda)^2 \Gamma(1-\lambda) \Gamma(1-2\lambda)^2 \Gamma(1-3\lambda)}{\Gamma(\lambda+1) \Gamma(2-4\lambda)}. \quad (37)$$

This result corresponds to the quantity M_1 in [24] which is the simplest basis element for the computation of massive three-loop diagrams in a general three-loop topology considered in [24]. We obtain agreement with [24].

2.6 The spectral density

From the physical point of view the interesting part of the analysis of sunrise-type diagrams is the construction of the spectral decomposition of the diagrams. For the two-point correlation function we determine the discontinuity across the physical cut in the complex plane of the squared momentum, $p^2 = -m^2 \pm i0$. Taking for instance the $n = 2$ sunrise-type diagram with two different masses m_1, m_2 in arbitrary dimensions, in (Euclidean) momentum space given by

$$\begin{aligned}\tilde{\Pi}(p) &= \int \frac{d^D k}{(2\pi)^D} \frac{1}{(k^2 + m_1^2)((k+p)^2 + m_2^2)} = \dots \\ &= \frac{\Gamma(1-\lambda)}{(4\pi)^{\lambda+1}} \int_0^1 \left(x(1-x)p^2 - (1-x)m_1^2 + xm_2^2 \right)^{\lambda-1} dx,\end{aligned}\quad (38)$$

the physical cut has influence on the integral for $x(1-x)p^2 + (1-x)m_1^2 + xm_2^2 < 0$. With $p^2 = -se^{\mp i\pi}$ we can calculate the discontinuity to obtain

$$\text{Disc} \left(x(1-x)p^2 + (1-x)m_1^2 + xm_2^2 \right)^{\lambda-1} = \frac{2\pi i (x(1-x)s - (1-x)m_1^2 - xm_2^2)^{\lambda-1}}{\Gamma(\lambda)\Gamma(1-\lambda)} \quad (39)$$

for $x_1 \leq x \leq x_2$ where x_1 and x_2 are the two zeros of the integrand which can be decomposed into $s^{\lambda-1}(x_2-x)^{\lambda-1}(x-x_1)^{\lambda-1}$. The spectral density is given by the discontinuity divided by $2\pi i$. Therefore, we finally obtain

$$\rho(s) = \frac{\Omega_{2\lambda+1}}{4\sqrt{s}(2\pi)^{2\lambda+1}} \left(\frac{(s - m_1^2 - m_2^2)^2 - 4m_1^2 m_2^2}{4s} \right)^{\lambda-1/2} \quad (40)$$

where $\Omega_d = 2\pi^{d/2}/\Gamma(d/2)$ is the volume of the unit sphere in d -dimensional space-time. Eq. (40) is of need in the following which is the reason why I have given some details about the calculation. In the third lecture we will see that configuration space technique allows for some other efficient tool for determining the spectral density, namely by inverting the so-called K -transform. In the next lecture I will continue with today's examples and give recurrence relations which allow to reduce the result to a finite set of master integrals, expressible in terms of transcendental numbers.

3 Recurrence relations and transcendental numbers

I continue the previous lecture by introducing just three other examples for calculating an sunrise-type diagram with the help of configuration space techniques in order to compare them with results in the literature. A wide field of diagrams to compare with is a subclass of three-loop bubbles B_N [24], namely

$$B_N(0, 0, n_3, n_4, n_5, n_6) = \int \frac{d^D k \, d^D l \, d^D p}{m^{3D} (\pi^{D/2} \Gamma(3 - D/2))^3} \times \\ \times \frac{m^{2n_3}}{((p+k)^2 + m^2)^{n_3}} \frac{m^{2n_4}}{((p+l)^2 + m^2)^{n_4}} \frac{m^{2n_5}}{((p+k+l)^2 + m^2)^{n_5}} \frac{m^{2n_6}}{(p^2 + m^2)^{n_6}} \quad (41)$$

with two propagators absent ($n_1 = n_2 = 0$). Actually we choose the remaining indices n_3, n_4, n_5 , and n_6 in a way that the results become finite, but we not only calculate the finite part but also the part proportional to ε in order to compare with [24]. Written in configuration space, the particular subset of bubble diagrams B_N is given by

$$B_N(0, 0, n_3, n_4, n_5, n_6) = \frac{2(64\pi^4)^{2-\varepsilon}}{(\Gamma(1+\varepsilon))^3 \Gamma(2-\varepsilon)} m^{2(n_3+n_4+n_5+n_6)-12+6\varepsilon} \times \\ \times \int_0^\infty D^{(n_3-1)}(x, m) D^{(n_4-1)}(x, m) D^{(n_5-1)}(x, m) D^{(n_6-1)}(x, m) x^{2\lambda+1} dx. \quad (42)$$

It is obvious that we end up with integrals of products of four Bessel functions with non-integer indices and a non-integer power of x . The plan for today's lecture is as follows: After introducing the results for the three examples in terms of these integrals, I will show that at least the expansion up to first order in ε is possible analytically. I will then introduce a reduction procedure in order to reduce the integrals to a basic set of two master integrals,

$$L_4(r) := \int_0^\infty (K_0(\xi))^4 \xi^r d\xi \quad \text{and} \quad L_4^l(r) := \int_0^\infty (K_0(x))^4 \xi^r \ln(e^{\gamma_E} \xi/2) dx \quad (43)$$

and will add considerations on the general class of basic integrals $L_n(r)$ and $L_n^l(r)$.

3.1 The example $B_N(0, 0, 2, 2, 2, 2)$

We start with the example which is represented by the central diagram in Fig. 2. Each of the lines is modified (indicated by the dots on the lines) which means that instead of the

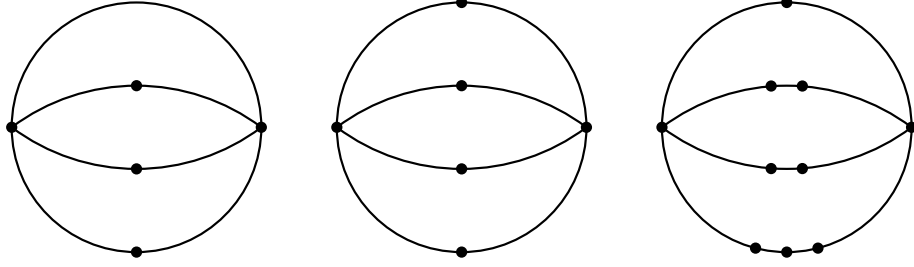


Figure 2: The diagrams for $B_N(0, 0, 2, 2, 2, 1)$, $B_N(0, 0, 2, 2, 2, 2)$, and $B_N(0, 0, 2, 3, 3, 4)$.

propagators $D(x, m)$ we have to use

$$D'(x, m) = \int \frac{d^D p}{(2\pi)^D} \frac{e^{ip_\mu x^\mu}}{(p^2 + m^2)^2} = \frac{(x/m)^{1-\lambda}}{2(2\pi)^{\lambda+1}} K_{\lambda-1}(mx) = \frac{(x/m)^\varepsilon}{2(2\pi)^{2-\varepsilon}} K_{-\varepsilon}(mx) \quad (44)$$

and obtain ($\xi = mx$)

$$B_N(0, 0, 2, 2, 2, 2) = \frac{2^{1-2\varepsilon}}{(\Gamma(1+\varepsilon))^3 \Gamma(2-\varepsilon)} \int_0^\infty (K_{-\varepsilon}(\xi))^4 \xi^{3+2\varepsilon} d\xi. \quad (45)$$

We now can use the general formula [65]

$$\left[\frac{\partial K_\nu(z)}{\partial \nu} \right]_{\nu=\pm n} = \pm \frac{1}{2} n! \sum_{k=0}^{n-1} \left(\frac{z}{2} \right)^{k-n} \frac{K_k(z)}{k!(n-k)}, \quad n \in \{0, 1, \dots\} \quad (46)$$

to expand the Bessel function in a series with respect to its index. In case of $K_{-\varepsilon}(z)$, however, the first derivative vanishes and we obtain $K_{-\varepsilon}(z) = K_0(z) + O(\varepsilon^2)$. Therefore, in expanding

$$\begin{aligned} \frac{2^{1-2\varepsilon} (K_{-\varepsilon}(\xi))^4 \xi^{3+2\varepsilon}}{(\Gamma(1+\varepsilon))^3 \Gamma(2-\varepsilon)} &= 2 (K_0(\xi))^4 \xi^3 \left(1 + (1 + 2\gamma_E - 2 \ln 2 + 2 \ln \xi) \varepsilon + O(\varepsilon^2) \right) = \\ &= 2 (K_0(\xi))^4 \xi^3 \left(1 + (1 + 2 \ln(e^{\gamma_E} \xi/2)) \varepsilon + O(\varepsilon^2) \right) \end{aligned} \quad (47)$$

we obtain

$$\begin{aligned} B_N(0, 0, 2, 2, 2, 2) &= 2(1+\varepsilon) \int_0^\infty (K_0(\xi))^4 \xi^3 d\xi + 4\varepsilon \int_0^\infty (K_0(\xi))^4 \xi^3 \ln(e^{\gamma_E} \xi/2) d\xi = \\ &= 2(1+\varepsilon) L_4(3) + 4\varepsilon L_4^l(3). \end{aligned} \quad (48)$$

In comparing with the analytical result in [24] we checked numerically [15]

$$\begin{aligned} I_4(3) &= -\frac{3}{16} + \frac{7}{32} \zeta(3), \\ I_4^l(3) &= \frac{3}{32} + \frac{3}{4} \text{Li}_4\left(\frac{1}{2}\right) - \frac{17\pi^4}{1920} - \frac{\pi^2}{32} (\ln 2)^2 + \frac{1}{32} (\ln 2)^4 + \frac{49}{128} \zeta(3). \end{aligned} \quad (49)$$

3.2 The example $B_N(0, 0, 2, 2, 2, 1)$

In the diagram on the left hand side of Fig. 2 one of the lines is not modified. Therefore, we have to deal with one regular propagator factor

$$D^{(0)}(x, m) = D(x, m) = \frac{(x/m)^{-\lambda}}{(2\pi)^{\lambda+1}} K_\lambda(mx) = \frac{(x/m)^{\varepsilon-1}}{(2\pi)^{2-\varepsilon}} K_{1-\varepsilon}(mx). \quad (50)$$

In this case we obtain

$$B_N(0, 0, 2, 2, 2, 1) = \frac{2^{2-2\varepsilon}}{(\Gamma(1+\varepsilon))^3 \Gamma(2-\varepsilon)} \int_0^\infty (K_{-\varepsilon}(\xi))^3 K_{1-\varepsilon}(\xi) \xi^{2+2\varepsilon} d\xi. \quad (51)$$

Using Eq. (46), we obtain

$$K_{1-\varepsilon}(\xi) = K_1(\xi) - \frac{\varepsilon}{\xi} K_0(\xi) + O(\varepsilon^2) \quad (52)$$

and

$$\frac{2^{2-2\varepsilon} (K_{-\varepsilon}(\xi))^3 K_{1-\varepsilon}(\xi) \xi^{2+2\varepsilon}}{(\Gamma(1+\varepsilon))^3 \Gamma(2-\varepsilon)} = 4\xi^2 \left(1 + \left(1 - \frac{1}{\xi} + \ln(e^{\gamma_E} \xi/2) \right) \varepsilon + O(\varepsilon^2) \right). \quad (53)$$

The result reads

$$\begin{aligned} B(0, 0, 2, 2, 2, 1) &= 4(1+\varepsilon) \int_0^\infty (K_0(\xi))^3 K_1(\xi) \xi^2 d\xi - 4\varepsilon \int_0^\infty (K_0(\xi))^4 \xi d\xi + \\ &\quad + 8\varepsilon \int_0^\infty (K_0(\xi))^3 K_1(\xi) \xi^2 \ln(e^{\gamma_E} \xi/2) d\xi. \end{aligned} \quad (54)$$

This result is not yet written in terms of $L_4(r)$ and $L_4^l(r)$ and will be treated after having introduced the reduction procedure.

3.3 The example $B_N(0, 0, 2, 3, 3, 4)$

In order to demonstrate the power of the configuration space technique also in this calculation, we finally choose the example found on the right hand side of Fig. 2, where the modified propagators

$$D^{(2)}(x, m) = \frac{(x/m)^{1+\varepsilon}}{8(2\pi)^{2-\varepsilon}} K_{-1-\varepsilon}(mx), \quad D^{(3)}(x, m) = \frac{(x/m)^{2+\varepsilon}}{48(2\pi)^{2-\varepsilon}} K_{-2-\varepsilon}(mx) \quad (55)$$

are used, together with the expansions

$$K_{-1-\varepsilon}(\xi) = K_1(\xi) + \frac{\varepsilon}{\xi} K_0(\xi) + O(\varepsilon^2), \quad K_{-2-\varepsilon}(\xi) = K_2(x) + \frac{2\varepsilon}{\xi} K_1(x) + \frac{2\varepsilon}{\xi^2} K_0(x) + O(\varepsilon^2). \quad (56)$$

We obtain

$$\begin{aligned}
B_N(0, 0, 2, 3, 3, 4) &= \frac{2^{-6-2\varepsilon}}{3(\Gamma(1+\varepsilon))^2\Gamma(2-\varepsilon)} \int_0^\infty K_{-\varepsilon}(\xi) (K_{-1-\varepsilon}(\xi))^2 K_{-2-\varepsilon}(\xi) \xi^{7+2\varepsilon} d\xi = \\
&= \frac{1+\varepsilon}{192} \int_0^\infty K_0(\xi) (K_1(\xi))^2 K_2(\xi) \xi^7 d\xi + \frac{\varepsilon}{96} \int_0^\infty K_0(\xi) (K_1(\xi))^2 K_2(\xi) \xi^6 d\xi + \\
&\quad + \frac{\varepsilon}{96} \int_0^\infty K_0(\xi) (K_1(\xi))^3 \xi^6 d\xi + \frac{\varepsilon}{96} \int_0^\infty (K_0(\xi))^2 (K_1(\xi))^2 \xi^5 d\xi + \\
&\quad + \frac{\varepsilon}{96} \int_0^\infty K_0(\xi) (K_1(\xi))^2 K_2(\xi) \xi^7 \ln(e^{\gamma_E} \xi/2) d\xi.
\end{aligned} \tag{57}$$

3.4 The reduction procedure

Especially in the last expression there are a lot of different integrals found which differ from the basis $L_4(r)$ and $L_4^l(r)$. However, the integrands can be reduced to integrand in terms of $K_0(\xi)$ and $K_1(\xi)$ only by using the relation

$$K_n(\xi) = 2\frac{n-1}{\xi}K_{n-1}(\xi) + K_{n-2}(\xi). \tag{58}$$

After the first step, namely the expansion of Bessel functions for non-integer indices, the above relation establishes the second step in our reduction procedure. Finally, we use

$$\begin{aligned}
\frac{d}{d\xi}K_0(\xi) &= -K_1(\xi) \quad \text{and} \\
\frac{d}{d\xi}K_1(\xi) &= -\frac{1}{2}(K_0(\xi) + K_2(\xi)) = -K_0(\xi) - \frac{1}{\xi}K_1(\xi)
\end{aligned} \tag{59}$$

to perform the third and last step, for instance

$$\begin{aligned}
L_4^{(1)}(r) &= \int_0^\infty (K_0(\xi))^3 K_1(\xi) \xi^r d\xi = - \int_0^\infty (K_0(\xi))^3 \frac{dK_0(\xi)}{d\xi} \xi^r d\xi = \\
&= - \left[K_0(\xi) (K_0(\xi))^3 \xi^r \right]_0^\infty + \int_0^\infty K_0(\xi) \frac{d}{d\xi} (K_0(\xi))^3 \xi^r d\xi = \\
&= 3 \int_0^\infty K_0(\xi) (K_0(\xi))^2 \frac{dK_0(\xi)}{d\xi} \xi^r d\xi + r \int_0^\infty K_0(\xi) (K_0(\xi))^3 \xi^{r-1} d\xi = \\
&= -3 \int_0^\infty (K_0(\xi))^3 K_1(\xi) \xi^r d\xi + r \int_0^\infty (K_0(\xi))^4 \xi^{r-1} d\xi
\end{aligned} \tag{60}$$

and therefore

$$L_4^{(1)}(r) = \int_0^\infty (K_0(\xi))^3 K_1(\xi) \xi^r d\xi = \frac{r}{4} \int_0^\infty (K_0(\xi))^4 \xi^{r-1} d\xi = \frac{r}{4} L_4(r-1). \tag{61}$$

The complete set of reduction formulas is given by

$$\begin{aligned}
L_4^{(4)}(r) &= (r-3)L_4^{(3)}(r-1) - 3L_4^{(2)}(r), \\
L_4^{(3)}(r) &= \frac{1}{2} \left((r-2)L_4^{(2)}(r-1) - 2L_4^{(1)}(r) \right), \\
L_4^{(2)}(r) &= \frac{1}{3} \left((r-1)L_4^{(1)}(r-1) - L_4(r) \right), \\
L_4^{(1)}(r) &= \frac{1}{4}rL_4(r-1),
\end{aligned} \tag{62}$$

$$\begin{aligned}
L_4^{l(4)}(r) &= (r-3)L_4^{l(3)}(r-1) + L_4^{(3)}(r-1) - 3L_4^{l(2)}(r), \\
L_4^{l(3)}(r) &= \frac{1}{2} \left((r-2)L_4^{l(2)}(r-1) + L_4^{(2)}(r-1) - 2L_4^{l(1)}(r) \right), \\
L_4^{l(2)}(r) &= \frac{1}{3} \left((r-1)L_4^{l(1)}(r-1) + L_4^{(1)}(r-1) - L_4^l(r) \right), \\
L_4^{l(1)}(r) &= \frac{1}{4} \left(rL_4^l(r-1) + L_4(r-1) \right),
\end{aligned} \tag{63}$$

in general

$$\begin{aligned}
L_n^{(m)}(r) &= \frac{1}{n-m+1} \left((r-m+1)L_n^{(m-1)}(r-1) - (m-1)L_n^{(m-2)}(r) \right), \\
L_n^{l(m)}(r) &= \frac{1}{n-m+1} \left((r-m+1)L_n^{l(m-1)}(r-1) + L_n^{(m-1)}(r-1) - (m-1)L_n^{l(m-2)}(r) \right)
\end{aligned} \tag{64}$$

and is coded in MATHEMATICA in order to automatically reduce to the master integrals [15]. The results for the examples after executing the second and third step of the recursion reads

$$\begin{aligned}
B_N(0, 0, 2, 2, 2, 2) &= 2(1+\varepsilon)L_4(3) + 4\varepsilon L_4^l(3) + O(\varepsilon^2), \\
B_N(0, 0, 2, 2, 2, 1) &= 2L_4(1) + 4\varepsilon L_4^l(1) + O(\varepsilon^2), \\
B_N(0, 0, 2, 3, 3, 4) &= \frac{1}{36}L_4(3) - \frac{1}{144}L_4(5) - \frac{1}{576}L_4(7) + O(\varepsilon).
\end{aligned} \tag{65}$$

Comparing with the results obtained by using the RECURSOR package [24],

$$\begin{aligned}
B_N(0, 0, 2, 2, 2, 2) &= -\frac{3}{8} + \frac{7}{16}\zeta(3) + O(\varepsilon), \\
B_N(0, 0, 2, 2, 2, 1) &= \frac{7}{4}\zeta(3) + O(\varepsilon), \\
B_N(0, 0, 2, 3, 3, 4) &= \frac{1}{576} + O(\varepsilon)
\end{aligned} \tag{66}$$

(the order ε is omitted here) we can adjust the master integrals

$$L_4(3) = -\frac{3}{16} + \frac{7}{32}\zeta(3), \quad L_4(1) = \frac{7}{8}\zeta(3), \quad 16L_4(3) - 2L_4(5) - L_4(7) = 1. \quad (67)$$

Especially the last relation is interesting because it means that

$$\int_0^\infty K_0(\xi) (K_1(\xi))^2 K_2(\xi) \xi^7 d\xi = \frac{1}{3}. \quad (68)$$

This surprising identity has been checked numerically as well. Note that only $L_4(r)$ for odd values of r are needed for the leading order contribution. However, before concentrating on the master integrals themselves, let me add some remarks on the efficiency of the reduction.

3.5 The efficiency of the reduction

Taking N to be the maximal total power of denominator factors, the calculation of a three-loop integral like in the previous examples would create and deserve a field of N^3 integrals which are recursively defined by each other using recurrence relations [24]. In contrast to this, the reduction procedure in our case needs N steps to reduce the result to a basis of $2[N/2] - 5$ basic elements $L_4(r)$ and $L_4^l(r)$. Therefore, the “costs” of our method are of the order N^2 which considerably reduces the time consumption in a computer evaluation.

3.6 Values for the master integrals

By comparing the results for different sun-rise type diagrams obtained by using our reduction method [15] and the procedure RECURSOR in [24] we can find values for the master integrals. The first results read

$$L_4(1) = \frac{7}{8}\zeta(3), \quad L_4(3) = \frac{7}{32}\zeta(3) - \frac{3}{16}, \quad L_4(5) = \frac{49}{128}\zeta(3) - \frac{27}{64}, \quad \dots \quad (69)$$

In general we found that the (odd-valued) master integrals are given by expressions of the kind $L_4(2r+1) = A_r\zeta(3) - B_r$. Of course we might ask whether there is a general way to calculate these master integrals. At least we can execute the calculation for the master $L_4(1)$. This master integral is (by a fresh view, i.e. not considering where the

master integral comes from) given by the three-loop sunrise-type bubble in two space-time dimensions (i.e. $\lambda = 0$),

$$\tilde{\Pi}(0) = \frac{2\pi^{\lambda+1}}{\Gamma(\lambda+1)} \int_0^\infty \left(\frac{(mx)^\lambda K_\lambda(mx)}{(2\pi)^{\lambda+1} x^{2\lambda}} \right)^4 x^{2\lambda+1} dx = \frac{1}{(2\pi)^3 m^2} \int_0^\infty (K_0(\xi))^4 \xi d\xi. \quad (70)$$

$\tilde{\Pi}(0)$ itself can be written as the two-dimensional integral over the product of two two-line correlators of the kind

$$\tilde{\Pi}_2(p) = \frac{1}{2\pi \sqrt{p^2} \sqrt{p^2 + 4m^2}} \ln \left(\frac{\sqrt{p^2 + 4m^2} + \sqrt{p^2}}{\sqrt{p^2 + 4m^2} - \sqrt{p^2}} \right) = \frac{1}{4\pi m^2} \frac{\tau}{\sinh \tau} \quad (71)$$

(the last identity for substituting $p = 2m \sinh(\tau/2)$), so that

$$L_4(1) = (2\pi)^3 m^2 \int \frac{d^2 p}{(2\pi)^2} \left(\tilde{\Pi}_2(p) \right)^2 = \frac{1}{4} \int_0^\infty \frac{\tau^2 d\tau}{\sinh \tau} = \frac{7}{8} \zeta(3) \quad (72)$$

where [64]

$$\int_0^\infty \frac{\tau^{\alpha-1} d\tau}{\sinh \tau} = \frac{2^\alpha - 1}{2^{\alpha-1}} \Gamma(\alpha) \zeta(\alpha) \quad (73)$$

has been used. The expression for general (odd) values for r reads

$$L_4(2r+1) = 2\pi m^2 \int \tilde{\Pi}(p) \left(-m^2 \square_p \right)^r \tilde{\Pi}_2(p) d^2 p \quad (74)$$

where $\square_p = \partial^2 / \partial p_\mu \partial p^\mu$ is the two-dimensional d'Alembert operator in (Euclidean) momentum space. It is still an open question whether this integral can be calculated to obtain the simple expression containing rationals and $\zeta(3)$. However, a closer look at the numerical value shows that, apart from the chance to obtain an analytical result, the attempt might not be worth the effort. Indeed, looking at the master integrals for higher and higher values of r we find that the contributions $A_r \zeta(3)$ and B_r increase while the difference leads to a significant cancellation, for $I_4(11)$ for instance up to three significant figures. Instead of trying to calculate the analytical expression, we therefore look for an asymptotic expansion of the integral at large values of r ,

$$L_4(2r+1) = \frac{\pi^2 \Gamma(2r)}{4^{2r+1}} \left(1 - \frac{1}{r-1/2} + O(1/r^2) \right). \quad (75)$$

We can introduce a new parameter κ which accounts for higher order terms in the asymptotic expansion. The expression

$$L_4(2r+1) = \frac{\pi^2 \Gamma(2r)}{4^{2r+1}} \left(1 + \frac{1}{r+\kappa} \right) \quad (76)$$

with $\kappa = 0.97$ gives numerical results with an accuracy better than 1% for all $r \geq 1$, while for $r > 3$ the relative accuracy is better than 10^{-3} . A similar expression can be found for the logarithmic masters,

$$L_4^l(2r+1) = \frac{\pi\Gamma(2r)}{4^{2r+1}} (\Psi(2r) + \gamma_E - 3\ln 2) \left(1 - \frac{1}{r + \kappa_l}\right) \quad (77)$$

where $\Psi(z) = \Gamma'(z)/\Gamma(z)$ is the polygamma function or logarithmic derivative of the gamma function. For $\kappa_l = 1.17$ the accuracy for $r > 3$ is better than 1%, for $r > 5$ better than 10^{-3} .

3.7 Back to the genuine sunset

As it is already visible in Eq. (64), the recurrence relations just discussed for $n = 4$ massive internal lines are given for other numbers of internal lines as well with no costs. We could for instance return to the genuine sunset with $n = 3$. In this case the master integral $L_3(1)$ is given by a two-loop sunset-type bubble in two space-time dimensions,

$$\tilde{\Pi}(0) = \frac{2\pi^{\lambda+1}}{\Gamma(\lambda+1)} \int_0^\infty \left(\frac{(mx)^\lambda K_\lambda(mx)}{(2\pi)^{\lambda+1} x^{2\lambda}} \right)^3 x^{2\lambda+1} dx = \frac{1}{(2\pi)^2 m^2} \int_0^\infty (K_0(\xi))^3 \xi d\xi \quad (78)$$

and, therefore ($t = e^{-\tau}$),

$$L_3(1; M/m) = m^2 \int \frac{\tilde{\Pi}_2(p)}{p^2 + M^2} d^2 p = \int_0^\infty \frac{m^2 \tau d\tau}{4m^2 \sinh^2(\tau/2) + M^2} = - \int_0^1 \frac{\ln t dt}{1 - 2\gamma t + t^2} \quad (79)$$

where the mass M of the third line is kept different from the other two masses m for a while. By differentiating with respect to M , any positive power of the propagator (and/or power in x in configuration space) can be obtained – therefore, all master integrals. Because of $\gamma = 1 - M^2/2m^2$, the denominator has two roots $t_{1,2} = \gamma \pm \sqrt{\gamma^2 - 1}$ with $t_1 t_2 = 1$, and we obtain

$$L_3(1; M/m) = - \int_0^1 \frac{\ln t dt}{(t - t_1)(t - t_2)} = - \frac{\text{Li}_2(1/t_1) - \text{Li}_2(1/t_2)}{t_1 - t_2} = \frac{\text{Li}_2(t_1) - \text{Li}_2(t_2)}{t_1 - t_2} \quad (80)$$

where $\text{Li}_2(z)$ is the dilogarithm function. The differentiation with respect to M is now straightforward and can be performed with a symbolic manipulation program. The pseudo-threshold case $M = 2m$ is a degenerate case, we obtain

$$L_3(1; 2) = - \int_0^1 \frac{\ln t dt}{(1+t)^2} = \ln 2 \quad (81)$$

while for $M = m$ we obtain $\gamma = 1/2$, $t_{1,2} = \exp(\pm i\pi/3)$, and therefore

$$L_3(1) = L_3(1; 1) = - \int_0^1 \frac{\ln t \, dt}{1 - t + t^2} = \frac{2}{\sqrt{3}} \text{Im} \text{Li}_2(e^{i\pi/3}) = \frac{2}{\sqrt{3}} \text{Cl}_2\left(\frac{\pi}{3}\right), \quad (82)$$

a result in terms of Clausen's dilogarithms.

3.8 Generalization to the spectacle topology

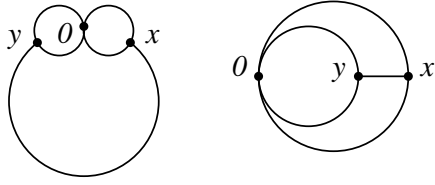


Figure 3: “spectacle+propagator” representation, also called “spectacle” topology diagram, in two different forms. The configuration space points 0 , x and y are indicated.

To finish today's lecture, we can look a bit beyond the rim of the plate of sunrise-type diagrams. Actually, we can generalize the configuration space technique to the so-called spectacle topology, as shown in Fig. 3 in two different representations. The configuration space expression of a spectacle topology diagram (again with a different mass M on the frame) written in a form suitable for the actual purpose is given by

$$S(M) = \int D(x - y, M) D(x, m)^2 D(y, m)^2 d^D x d^D y. \quad (83)$$

The key relation for a significant simplification of the configuration space integral with spectacle topology is given by a relation obtained from the addition theorem of Bessel functions [65]. I will not go into detail here, only mention the result [15]

$$\int \frac{K_\lambda(|r - \rho|)}{(2\pi)^{\lambda+1} |r - \rho|^\lambda} d\Omega_\rho = \frac{I_\lambda(\rho)}{\rho^\lambda} \frac{K_\lambda(r)}{r^\lambda}, \quad r > \rho \quad (84)$$

where $I_\lambda(z)$ is the modified Bessel function of the first kind. This result allows one to write

$$\begin{aligned} S(M) &= \int \frac{M^{2\lambda}}{(2\pi)^{\lambda+1}} \frac{K_\lambda(M|x - y|)}{(M|x - y|)^\lambda} D(x, m)^2 D(y, m)^2 d^D x d^D y = \\ &= \left(\frac{2\pi^{\lambda+1}}{\Gamma(\lambda + 1)} \right)^2 M^{2\lambda} \int_0^\infty (D(x, m))^2 x^{2\lambda+1} dx \int_0^\infty (D(y, m))^2 y^{2\lambda+1} dy \times \\ &\quad \times \left(\frac{K_\lambda(Mx)}{(Mx)^\lambda} \frac{I_\lambda(My)}{(My)^\lambda} \theta(x - y) + \frac{K_\lambda(My)}{(My)^\lambda} \frac{I_\lambda(Mx)}{(Mx)^\lambda} \theta(y - x) \right). \end{aligned} \quad (85)$$

As an illustration we look at the two-dimensional space-time where

$$S(M) = \frac{1}{(2\pi)^2} \int_0^\infty x (K_0(mx))^2 dx \int_0^\infty y (K_0(my))^2 dy \times \\ \times (K_0(Mx)I_0(My)\theta(x-y) + K_0(My)I_0(Mx)\theta(y-x)), \quad (86)$$

comparing this result with the momentum space representation

$$S(M) = \int \frac{d^2p}{(2\pi)^2} \frac{(\tilde{\Pi}_2(p))^2}{p^2 + M^2} = \frac{2\pi}{m^4} \int_0^1 \frac{t \ln^2 t dt}{(1-t^2)(1-2\gamma t + t^2)} \quad (87)$$

where the same chain of substitutions have been used. We obtain

$$S(M) = \frac{f(t_1) - f(t_2)}{t_1 - t_2}, \quad f(t) = \frac{4\pi t \text{Li}_3(1/t) - (t+7)\zeta(3)}{m^4(t^2 - 1)} \quad (88)$$

where $\text{Li}_3(z)$ is the trilogarithm function. While for $M = m$ we obtain a result including the Clausen trilogarithm $\text{Cl}_3(2\pi/3)$, for the case $M = 2m$ the integral for $S(M = 2m)$ simplifies as in the case of the sunrise diagram, one obtains

$$S(2m) = \frac{\pi}{m^4} \left(\frac{7}{8} \zeta(3) - \ln 2 \right). \quad (89)$$

In all these cases the sixth order roots of unity ± 1 , $\exp(\pm\pi/3)$, and $\exp(\pm 2\pi/3)$ play an important role [67]. In [15, 25] we have followed the lines given in [67] and have constructed a shuffle algebra for the occurring integrals which finally lead to the transcendental numbers which normally occur in these calculations. At this point I will not go into detail. Instead I close the lecture by mentioning that the numerical comparison between the result obtained in the momentum space approach with the result within the configuration space technique show coincidence. Tomorrow we will deal with the consideration of sunrise-type diagrams close to threshold.

4 Expansions close to threshold

From the physical point of view the interesting part of our analysis of sunrise-type diagrams is the construction of the spectral decomposition of the diagram. Using the configuration space technique, the spectral density can be constructed directly from the correlator function in configuration space. The technique introduced in [13] is based on an integral transform. Starting with the dispersion relation in (Euclidean) momentum space,

$$\tilde{\Pi}(q) = \int_0^\infty \frac{\rho(s)ds}{q^2 + s} = \int_0^\infty \rho(s)\tilde{D}(q, \sqrt{s})ds, \quad (90)$$

the corresponding relation in configuration space reads

$$\Pi(x) = \int_0^\infty \rho(s)D(x, \sqrt{s})ds. \quad (91)$$

This representation was used for sum rule applications in [68, 69] where the spectral density for the two-loop sunrise diagram was found in two-dimensional space-time [70]. With the explicit form of the propagator in configuration space given by

$$D(x, \sqrt{s}) = \frac{(\sqrt{s}/x)^\lambda}{(2\pi)^{\lambda+1}} K_\lambda(\sqrt{s}x), \quad (92)$$

the representation turns into a particular example of the Hankel transform, namely the K -transform [71, 72]

$$g(y) = \int_0^\infty f(x)K_\nu(xy)\sqrt{xy}dx. \quad (93)$$

The inverse of this transform is known to be given by

$$f(x) = \frac{1}{i\pi} \int_{c-i\infty}^{c+i\infty} g(y)I_\nu(xy)\sqrt{xy}dy \quad (94)$$

where the vertical contour in the complex plane is placed to the right of the right-most singularity of the function $g(y)$ [72]. Translating this inverse K -transform to our situation which relates $\rho(s)$ and $\Pi(x)$, we obtain

$$\sqrt{s}^\lambda \rho(s) = -(2\pi)^\lambda i \int_{c-i\infty}^{c+i\infty} \Pi(x)x^{\lambda+1}I_\lambda(\sqrt{s}x)dx. \quad (95)$$

The inverse transform given in Eq. (95) solves the problem of determining the spectral density of sunrise-type diagrams by reducing it to the computation of a one-dimensional

integral for the general class of sunrise-type diagrams with any number of internal lines and different masses. Because the contour can bypass the area of small values of x , the integral is finite. Using this expression, the spectral density is known numerically as a function of s . Eq. (95) will be used in the following to compare the exact result with different types of expansions found in the literature, in order to test their convergence behaviour.

4.1 Considerations in Minkowskian domain

The threshold region of a sunrise-type diagram is determined by the condition $q^2 + M^2 \cong 0$, where q is the Euclidean momentum and $M = \sum_i m_i$ is the threshold value for the spectral density. We introduce the Minkowskian momentum p defined by $p^2 = -q^2$ which is an analytic continuation to the physical cut. Operationally, this analytic continuation can be performed by replacing $q \rightarrow ip$. To analyze the region near the threshold we use the parameter $\Delta = M - p$ which takes complex values, while in phenomenological applications the parameter $E = -\Delta = p - M$ is more convenient. The spectral density will be written as a function of E in the following, $\tilde{\rho}(E) = \rho((M + E)^2)$. The analytic continuation of the Fourier transform $\tilde{\Pi}(q)$ to the Minkowskian domain has the form

$$\tilde{\Pi}_M(p) = 2\pi^{\lambda+1} \int_0^\infty \left(\frac{ipx}{2}\right)^{-\lambda} J_\lambda(ipx) \Pi(x) x^{2\lambda+1} dx \quad (96)$$

(as we work in Minkowskian domain only, the index M will be dropped in the following).

4.2 Large x behaviour of the weight

For the threshold expansion we have to analyze the large x behaviour of the integrand. It is this region that saturates the integral in the limit $p \rightarrow M$ or, equivalently, $E \rightarrow 0$. It is convenient to perform the analysis in a basis where the integrand has a simple large x behaviour. The most important part of the integrand is the Bessel function $J_\lambda(ipx)$ which, however, contains both rising and falling branches at large x . It resembles the situation with the elementary trigonometric function $\cos(z)$ to which the Bessel function $J_\lambda(z)$ is

rather close in a certain sense, as we will see. $\cos(z)$ is a linear combination of exponentials,

$$\cos(z) = \frac{1}{2} (e^{iz} + e^{-iz}). \quad (97)$$

In the same manner, the Bessel function $J_\lambda(z)$ can be written as a sum of two Hankel functions $H_\lambda^\pm(z) = J_\lambda(z) \pm iY_\lambda(z)$,

$$J_\lambda(z) = \frac{1}{2} (H_\lambda^+(z) + H_\lambda^-(z)), \quad (98)$$

and for pure imaginary argument the Hankel functions show simple asymptotic behaviour

$$H_\lambda^\pm(iz) \sim z^{-1/2} e^{\pm z}. \quad (99)$$

Accordingly, we split up $\tilde{\Pi}(p)$ into $\tilde{\Pi}(p) = \tilde{\Pi}^+(p) + \tilde{\Pi}^-(p)$ with

$$\tilde{\Pi}^\pm(p) = \pi^{\lambda+1} \int_0^\infty \left(\frac{ipx}{2}\right)^{-\lambda} H_\lambda^\pm(ipx) \Pi(x) x^{2\lambda+1} dx. \quad (100)$$

The two parts $\tilde{\Pi}^\pm(p)$ of the polarization function $\tilde{\Pi}(p)$ have completely different behaviour near threshold and are analyzed independently in the following.

4.3 The polarization function $\tilde{\Pi}^+(p)$

The behaviour of $\tilde{\Pi}^+(p)$ for large x is given by the asymptotic form of the functions which I simply write up to the leading terms as

$$H^+(ipx) = \sqrt{\frac{2}{i\pi px}} e^{-px} (1 + O(x^{-1})), \quad K(mx) = \sqrt{\frac{\pi}{2mx}} e^{-mx} (1 + O(x^{-1})). \quad (101)$$

We conclude that the large x range of the integral (above a reasonably large cutoff parameter Λ) has the general form

$$\tilde{\Pi}_\Lambda^+(M - \Delta) \sim \int_\Lambda^\infty x^{-a} e^{-(2M-\Delta)x} dx, \quad a = (n-1)(\lambda + 1/2). \quad (102)$$

The right hand side is an analytic function in Δ in the vicinity of $\Delta = 0$. It exhibits no cut or other singularities near the threshold and therefore does not contribute to the spectral density. I could therefore go ahead to the second contribution $\tilde{\Pi}^-(p)$. However, I want

to do a bit more in order to fill $\tilde{\Pi}^+(p)$ with “life” (i.e., meaning). In using the relation

$$K_\lambda(z) = \frac{\pi i}{2} e^{i\lambda\pi/2} H_\lambda^+(iz) \quad (103)$$

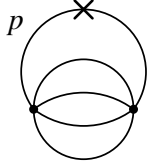


Figure 4: Representation of the regular part $\tilde{\Pi}^+(-p^2)$ as vacuum bubble with added line. The cross denotes an arbitrary number of derivatives of the specified line.

between Bessel functions of different kind I can replace the Hankel function $H_\lambda^+(ipx)$ by the Bessel function $K_\lambda(px)$. But since the propagator of a massive particle (massive line in the diagram) is given by the Bessel function $K_\lambda(mx)$ up to a power x , the weight function behaves like a propagator of an additional line with “mass” p . The explicit expression is given by (cf. Fig. 4)

$$\tilde{\Pi}^+(p) = \frac{(-2\pi i)^{2\lambda+1}}{(p^2)^\lambda} \int_0^\infty \Pi_+(x) x^{2\lambda+1} dx, \quad \Pi_+(x) = \Pi(x) D(x, p). \quad (104)$$

4.4 The polarization function $\tilde{\Pi}^-(p)$

In contrast to the previous case, the integrand of the part $\tilde{\Pi}^-(p)$ contains $H^-(ipx)$ which behaves like a rising exponential function at large x ,

$$H^-(ipx) \sim x^{-1/2} e^{px}. \quad (105)$$

Therefore, the integral has the large x behaviour

$$\tilde{\Pi}_\Lambda^-(M - \Delta) \sim \int_\Lambda^\infty x^{-a} e^{-\Delta x} dx. \quad (106)$$

The exponential factor $e^{-\Delta x}$ which establishes an effective inverse proportionality between Δ and x is the reason for the importance of the large x behaviour as being essential for the near threshold expansion of the spectral density. However, for $\Delta < 0$ the integral diverges at the upper limit, leading to non-analyticity at the threshold $\Delta = 0$. In the complex Δ plane with a cut along the negative real axis the integral is analytic. This cut corresponds to the physical positive energy cut. The discontinuity across the cut gives rise to the non-vanishing spectral density of the contribution $\tilde{\Pi}^-(p)$.

In order to obtain an expansion for the spectral density near the threshold in an analytical form we make use of the asymptotic series expansion for the function $\Pi(x)$ that crucially simplifies the integrands but still preserves the singular structure of the integral in terms of the variable Δ . Because of the already mentioned asymptotic expansion

$$K_\lambda^{\text{as}}(mx) = \sqrt{\frac{\pi}{2mx}} e^{-mx} \left(1 + O(x^{-1})\right), \quad (107)$$

the asymptotic expansion of the function $\Pi(x)$ consists of an exponential factor e^{-Mx} and an inverse power series in x up to an order \tilde{N} closely related to N . It is this asymptotic expansion that determines the singularity structure of the integral. We write the whole integral in the form of the sum of two terms again,

$$\begin{aligned} \tilde{\Pi}^-(p) &= \pi^{\lambda+1} \int \left(\frac{ipx}{2}\right)^{-\lambda} H_\lambda^-(ipx) (\Pi(x) - \Pi_N^{\text{as}}(x)) x^{2\lambda+1+2\varepsilon} dx + \\ &+ \pi^{\lambda+1} \int \left(\frac{ipx}{2}\right)^{-\lambda} H_\lambda^-(ipx) \Pi_N^{\text{as}}(x) x^{2\lambda+1+2\varepsilon} dx = \tilde{\Pi}^{di}(p) + \tilde{\Pi}^{as}(p). \end{aligned} \quad (108)$$

The integrand of the difference term $\tilde{\Pi}^{di}(p)$ behaves as $1/x^{\tilde{N}}$ at large x while the integrand of the second term accumulates all lower powers of the large x expansion. We will again consider the two parts in turn. However, a comment on the regularization is in order here.

4.5 Comment on the regularization used

Being interested only in the large x behaviour, we introduced a cutoff Λ which necessary at least at this point because the asymptotic expansions are not defined for small values of x and lead to divergences. However, from the practical point of view the calculation of the regularized integrals with an explicit cutoff is inconvenient. Instead, the standar way to cope with such a situation is to use dimensional regularization. Note that dimensional regularization does not necessarily regularize all divergences in this case (in contrast to the standard case of ultraviolet divergences) but nevertheless is sufficient for our purposes. Therefore, we use a parameter ε independent of λ to regularize the divergences at small x .

4.6 The difference part $\tilde{\Pi}^{di}(p)$

In $\tilde{\Pi}^{di}(p)$ the subtracted asymptotic series to order N cancels the inverse power behaviour of the integrand to this degree N . Therefore, the integrand decreases sufficiently fast for large values of x and the integral even converges for $\Delta = 0$. The part $\tilde{\Pi}^{di}(p)$ is regular and gives no contribution to the spectral density up to the order Δ^N .

4.7 The asymptotic part $\tilde{\Pi}^{as}(p)$

The integral $\tilde{\Pi}^{as}(p)$ is still rather complicated to compute. But we can go a step further in its analytical evaluation. Indeed, since the singular behaviour of $\tilde{\Pi}^{as}(p)$ is determined by the behaviour at large x , we can replace the first factor, i.e. the Hankel function, in the large x region by its asymptotic expansion up to some order N ,

$$H_{\lambda,N}^{-as}(iz) = \sqrt{\frac{2}{\pi z}} e^{z+i\lambda\pi/2} \left[\sum_{n=0}^{N-1} \frac{(-1)^n(\lambda, n)}{(2z)^n} + \theta \frac{(-1)^N(\lambda, N)}{(2z)^N} \right] \quad (109)$$

with

$$\theta \in [0, 1], \quad (\lambda, n) := \frac{\Gamma(\lambda + n - 1/2)}{n! \Gamma(\lambda - n - 1/2)} \quad (110)$$

to obtain the double asymptotic representation

$$\tilde{\Pi}^{das}(p) = \pi^{\lambda+1} \int_0^\infty \left(\frac{ipx}{2} \right)^{-\lambda} H_{\lambda,N}^{-as}(ipx) \Pi_N^{as}(x) x^{2\lambda+1+2\varepsilon} dx. \quad (111)$$

Both asymptotic expansions are straightforward and can be obtained from standard handbooks on Bessel functions. We therefore arrive at our final result: the integration necessary for evaluating the near threshold expansion of the sunrise-type diagrams reduces to integrals of Euler's Gamma function type, i.e. integrals containing exponentials and powers in the integrand. Indeed, the result of the asymptotic expansion of the integrand is an exponential function $e^{-\Delta x}$ times a power series in $1/x$, namely

$$x^{-a+2\varepsilon} e^{-\Delta x} \sum_{j=0}^{N-1} \frac{A_j}{x^j} \quad (112)$$

where $a = (n-1)(\lambda+1/2)$ has already been used earlier and the coefficients A_j are simple functions of the momentum p and the masses m_i . This expression can be integrated

analytically using

$$\int_0^\infty x^{-a+2\varepsilon} e^{-\Delta x} dx = \Gamma(1-a+2\varepsilon) \Delta^{a-1-2\varepsilon}. \quad (113)$$

The result is

$$\tilde{\Pi}^{das}(M-\Delta) = \sum_{j=0}^{N-1} A_j \Gamma(1-a-j+2\varepsilon) \Delta^{a+j-1-2\varepsilon}. \quad (114)$$

This expression is our final representation for the part of the polarization function of a sunrise-type diagram necessary for the calculation of the spectral density near the production threshold. Starting from this main result in Eq. (114), I discuss the general structure in some detail. In the case where a takes integer values, these coefficients result in $1/\varepsilon$ -divergences for small values of ε . The powers of Δ in Eq. (114) have to be expanded to first order in ε and give

$$\frac{1}{2\varepsilon} \Delta^{2\varepsilon} = \frac{1}{2\varepsilon} + \ln \Delta + O(\varepsilon). \quad (115)$$

Because of

$$\text{Disc } \ln(\Delta) \equiv \ln(-E-i0) - \ln(-E+i0) = -2\pi i \theta(E) \quad (116)$$

$\tilde{\Pi}^{das}(M-\Delta)$ in Eq. (114) contributes to the spectral density. For half-integer values of a the power of Δ itself has a cut even for $\varepsilon = 0$. The discontinuity is then given by

$$\text{Disc } \sqrt{\Delta} = -2i\sqrt{E} \theta(E). \quad (117)$$

Our method to construct a threshold expansion thus simply reduces to the analytical calculation of the part $\tilde{\Pi}^{das}(p)$ which can be done for arbitrary dimension and an arbitrary number of lines with different masses. In the next subsections I work out some specific examples which demonstrate both the simplicity and efficiency of our method.

4.8 First example: equal mass ($n = 3$) sunrise diagram

For the genuine sunrise diagram with equal masses (the last restriction for reasons of representation only), the double asymptotic expansion reads

$$\begin{aligned} \pi^2 \left(\frac{ipx}{2} \right)^{-1} H_{1,N}^{as}(px) \Pi_N^{as}(x) x^{3+2\varepsilon} &= \frac{m^{3/2} e^{(p-3m)x}}{(4\pi)^3 p^{3/2}} x^{-3+2\varepsilon} \times \\ &\times \left\{ 1 + \frac{9}{8mx} - \frac{3}{8px} + \frac{9}{128m^2 x^2} - \frac{27}{64mpx^2} - \frac{15}{128p^2 x^2} + O(x^{-3}) \right\}. \end{aligned} \quad (118)$$

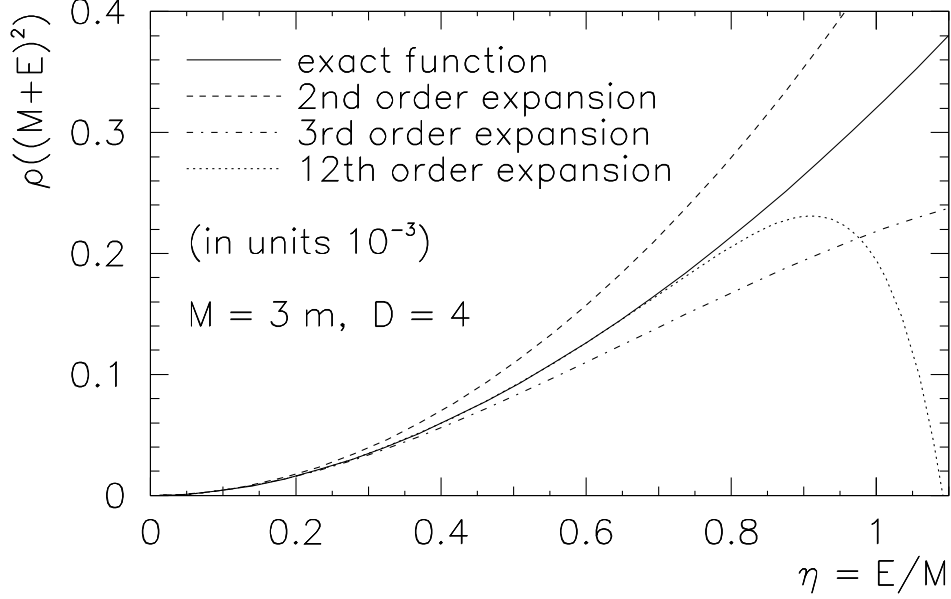


Figure 5: Various results for the spectral density for $n = 3$ equal masses in $D = 4$ space-time dimensions in dependence on the threshold parameter E/M . Shown are the exact solution obtained by using Eq. (95) (solid curve) and threshold expansions for different orders taken from Eq. (119) (dashed to dotted curves).

The spectral density is obtained by performing the term-by-term integration of the series and by evaluating the discontinuity across the cut along the positive energy axis $E > 0$. The result reads

$$\begin{aligned} \tilde{\rho}(E) = \frac{E^2}{384\pi^3\sqrt{3}} & \left\{ 1 - \frac{1}{2}\eta + \frac{7}{16}\eta^2 - \frac{3}{8}\eta^3 + \frac{39}{128}\eta^4 - \frac{57}{256}\eta^5 \right. \\ & \left. + \frac{129}{1024}\eta^6 - \frac{3}{256}\eta^7 - \frac{4047}{32768}\eta^8 + \frac{18603}{65536}\eta^9 - \frac{248829}{524288}\eta^{10} + O(\eta^{11}) \right\} \end{aligned} \quad (119)$$

where the notation $\eta = E/M$, $M = 3m$ is used [16]. The simplicity of this derivation is striking and easily reproduces the expansion coefficients in [10]. For different orders the result is compared with the exact result from inverse K -transform (Eq. (95)) in Fig. 5.

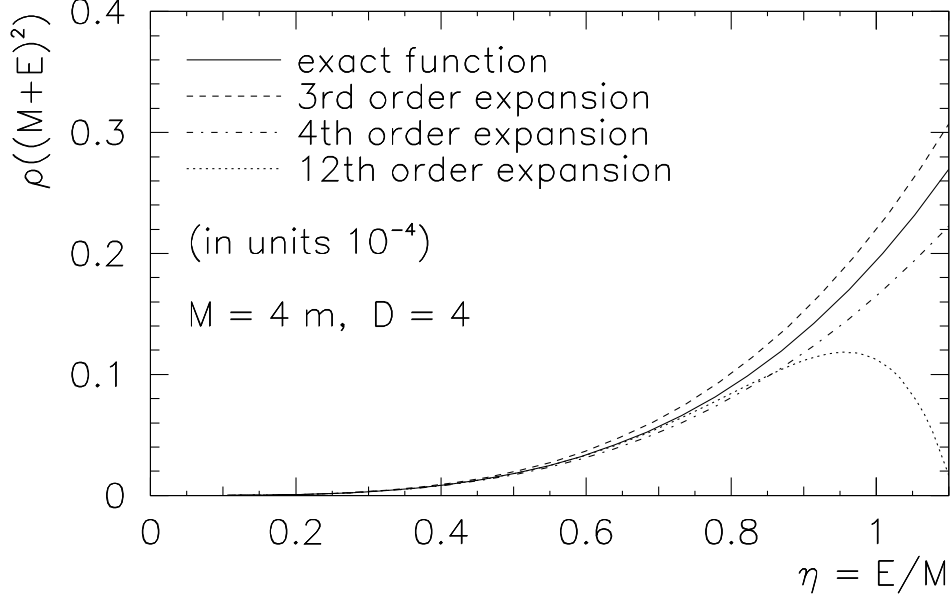


Figure 6: Various results for the spectral density for $n = 4$ equal masses in $D = 4$ space-time dimensions in dependence on the threshold parameter E/M . Shown are the exact solution obtained by using Eq. (95) (solid curve) and threshold expansions for different orders taken from Eq. (120) (dashed to dotted curves).

4.9 Second example: equal mass $n = 4$ sunrise-type diagram

The sunrise-type diagram with four or more propagators cannot be easily done by using the momentum space technique because it requires the multiloop integration of entangled momenta. Within the configuration space technique the generalization to any number of lines (or loops) is immediate by no effort. For the spectral density of the equal mass $n = 4$ sunrise-type diagram we obtain (cf. Fig. 6)

$$\begin{aligned} \tilde{\rho}(E) = \frac{E^{7/2}M^{1/2}}{26880\pi^5\sqrt{2}} \left\{ 1 - \frac{1}{4}\eta + \frac{81}{352}\eta^2 - \frac{2811}{18304}\eta^3 + \frac{17581}{292864}\eta^4 \right. \\ \left. + \frac{1085791}{19914752}\eta^5 - \frac{597243189}{3027042304}\eta^6 + \frac{4581732455}{12108169216}\eta^7 - \frac{496039631453}{810146594816}\eta^8 + O(\eta^9) \right\} \end{aligned} \quad (120)$$

where $\eta = E/M$ and $M = 4m$ is the threshold value. One sees the difference with the previous three-line case. In Eq. (120) the cut represents the square root branch while in the three-line case it was a logarithmic cut. This underlines my earlier considerations.

4.10 Strongly asymmetric mass arrangement

As we have seen, the threshold expansion for equal (or close) masses breaks down for $E \sim M = \sum m_i$. However, if the masses are not equal, the region of the breakdown of the expansion is determined by the mass with the smallest numerical value. Actually, one finds a breakdown at $E \sim 2m_0$ where m_0 is a mass much smaller than the others. To our best knowledge, this issue has not been touched earlier. In the following I will describe a technique called resummation of the smallest mass contribution [16]. Instead of the double asymptotic expansion we use the partial asymptotic expansion

$$\tilde{\Pi}^{pas}(p) = \pi^{\lambda+1} \int_0^\infty \left(\frac{ipx}{2}\right)^{-\lambda} H_{\lambda,N}^{-as}(ipx) \Pi_{m_0}^{as}(x) x^{2\lambda+1+2\varepsilon} dx \quad (121)$$

where the asymptotic expansions are substituted for all propagators except for the one with the smallest mass m_0 ,

$$\Pi_{m_0}^{as}(x) = \Pi_{n-1}^{as}(x) D(m_0, x). \quad (122)$$

Because of the knowledge of

$$\begin{aligned} \int_0^\infty x^{\mu-1} e^{-\tilde{\alpha}x} K_\nu(\beta x) dx &= \\ &= \frac{\sqrt{\pi}(2\beta)^\nu}{(2\tilde{\alpha})^{\mu+\nu}} \frac{\Gamma(\mu+\nu)\Gamma(\mu-\nu)}{\Gamma(\mu+1/2)} {}_2F_1\left(\frac{\mu+\nu}{2}, \frac{\mu+\nu+1}{2}; \mu+\frac{1}{2}; 1-\frac{\beta^2}{\tilde{\alpha}^2}\right) \end{aligned} \quad (123)$$

with $\tilde{\alpha} = \Delta - m_0$ and $\beta = m_0$, $\tilde{\Pi}^{pas}(p)$ is expressible in terms of hypergeometric functions [73]. The same is valid for the spectral density, because

$$\begin{aligned} \frac{1}{2\pi i} \text{Disc} \int_0^\infty x^{\mu-1} e^{\alpha x} K_\nu(\beta x) dx &= \\ &= \frac{2^\mu (\alpha^2 - \beta^2)^{1/2-\mu}}{\alpha^{1/2-\nu} \beta^\nu} \frac{\Gamma(3/2)}{\Gamma(3/2-\mu)} {}_2F_1\left(\frac{1-\mu-\nu}{2}, \frac{2-\mu-\nu}{2}; \frac{3}{2}-\mu; 1-\frac{\beta^2}{\alpha^2}\right) \end{aligned} \quad (124)$$

where $\alpha = E + m_0$. For the case of an $n = 2$ sunrise-type diagram with masses m and $m_0 \ll m$ we compare the exact result in Eq. (95) for the spectral density with the pure expansion near threshold

$$\begin{aligned} \tilde{\rho}^{das}(E) &= \frac{\sqrt{2m_0 m E}}{8\pi^2 M^{3/2}} \left\{ 1 + \left(\frac{1}{m} + \frac{1}{m_0} - \frac{7}{M} \right) \frac{E}{4} \right. \\ &\quad \left. - \left(\frac{1}{m_0^2} + \frac{1}{m^2} + \frac{12}{m_0 m} - \frac{79}{M^2} \right) \frac{E^2}{32} + O(E^3) \right\} \end{aligned} \quad (125)$$

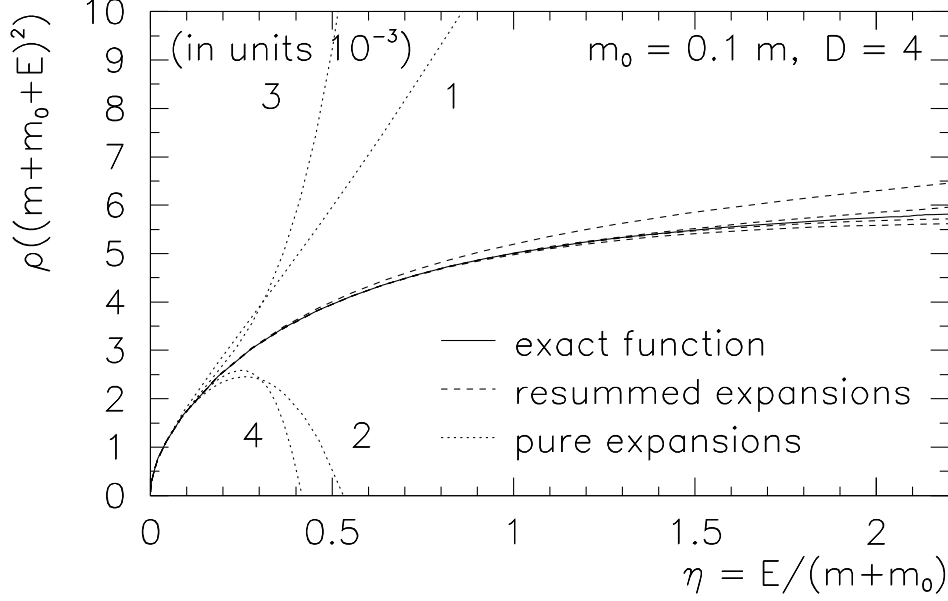


Figure 7: Various solutions for the spectral density for two masses m and $m_0 \ll m$ and $D = 4$ space-time dimensions. Shown are the exact solution which is obtained by using Eq. (95) (solid curve), the pure threshold expansions using Eq. (125) (dotted curves), and the solutions for the resummation of the smallest mass contributions like in Eq. (126) (dashed curves), both expansions from the first up to the fourth order in the asymptotic expansion. For the pure threshold expansion the order is indicated explicitly.

($M = m + m_0$, the second order asymptotic expansion should suffice to show the general features in a short and concise form) with the resummed result

$$\begin{aligned} \tilde{\rho}^{pas}(E) = & \frac{\sqrt{mE(E+2m_0)}}{8\pi^2(E+M)^{3/2}} \left\{ {}_2F_1 \left(0, \frac{1}{2}; \frac{3}{2}; 1 - \frac{m_0^2}{(E+m_0)^2} \right) \right. \\ & + \frac{E(E+2m_0)}{8m(E+M)} {}_2F_1 \left(\frac{1}{2}, 1; \frac{5}{2}; 1 - \frac{m_0^2}{(E+m_0)^2} \right) \\ & \left. - \frac{E^2(E+2m_0)^2}{128m^2(E+M)^2} \left(1 + \frac{16m(E+M)}{5(E+m_0)^2} \right) {}_2F_1 \left(1, \frac{3}{2}; \frac{7}{2}; 1 - \frac{m_0^2}{(E+m_0)^2} \right) + \dots \right\}. \end{aligned} \quad (126)$$

Having used $\varepsilon = 0$ for the finite spectral density, the first term in curly braces of Eq. (126) is obviously equal to 1 in this limit because the first parameter of the hypergeometric function vanishes. However, I keep Eq. (126) in its given form to show the structure of

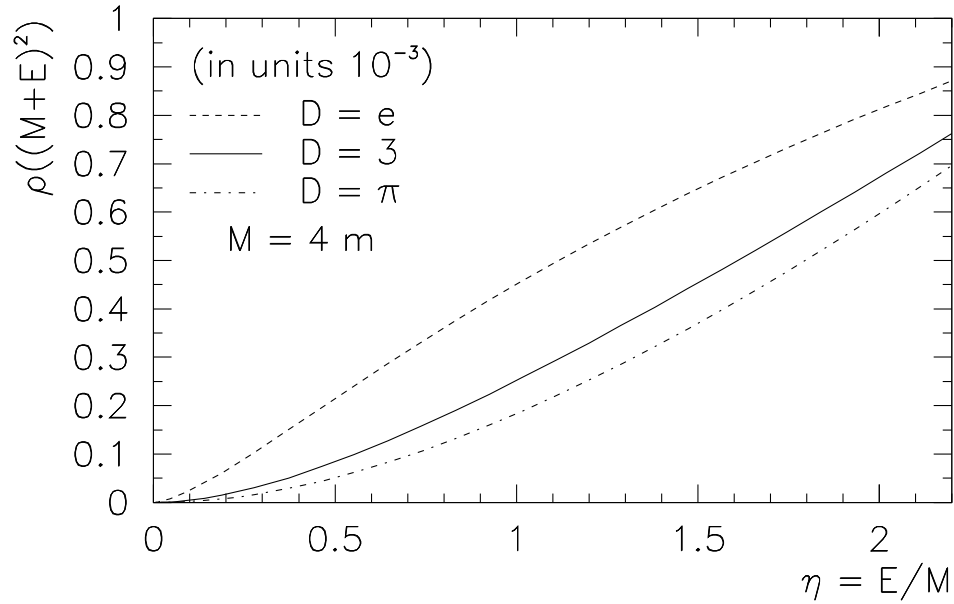


Figure 10: The spectral density for the four-line sunrise-type diagram with equal masses for $D = e = 2.718\dots$, $D = 3$, and $D = \pi = 3.14\dots$ space-time dimensions, to demonstrate the practical convenience of the method.

the contributions. The result of the comparison is shown in Fig. 7. The convergence of different orders of resummed expansions is remarkable, while the pure expansion diverges already at an early stage.

4.11 A last diagram

The last figure I want to show is a funny one. In order to demonstrate the universality of the configuration space method, in Fig. 10 I show the spectral density for the $n = 4$ sunrise-type diagram obtained via the inverse K -transform in Eq. (95) for the space-time dimensions $D = e = 2.718\dots$, $D = 3$, and $D = \pi = 3.14\dots$.

Acknowledgements

At this point I want to thank the organizers of this conference for the interesting and challenging opportunity to give a lecture series about the subject I'm already working on since long. I enjoyed the interesting comments and discussions during or after my lectures and the stimulating atmosphere of the conference in general. I want to thank my collaborators Jürgen Körner and Alexei Pivovarov for the ongoing work on this subject. My work is supported by the DFG, Germany via the Graduiertenkolleg "Eichtheorien" in Mainz.

References

- [1] A.G. Grozin, Nucl. Instrum. Meth. **A502** (2003) 815
- [2] P. Mastrolia and E. Remiddi, "Analytic evaluation of Feynman graph integrals", [arXiv:hep-ph/0211210]
- [3] P. Mastrolia and E. Remiddi, Nucl. Phys. **B657** (2003) 397
- [4] H. Czyż, A. Grzeńska and R. Zabawa, Phys. Lett. **B538** (2002) 52
- [5] Y. Schröder, "Automatic reduction of four-loop bubbles", [arXiv:hep-ph/0211288]
- [6] F.A. Berends, M. Buza, M. Böhm and R. Scharf, Z. Phys. **C63** (1994) 227
- [7] P. Post and K. Schilcher, Phys. Rev. Lett. **79** (1997) 4088
- [8] P. Post and J.B. Tausk, Mod. Phys. Lett. **A11** (1996) 2115
- [9] A.K. Rajantie, Nucl. Phys. **B480** (1996) 729; **B513** (1998) 761(E)
- [10] F.A. Berends, A.I. Davydychev and N.I. Ussyukina, Phys. Lett. **B426** (1998) 95
- [11] J. Gasser and M.E. Sainio, Eur. Phys. J. **C6** (1999) 297

- [12] E. Mendels, *Nuovo Cim.* **A45** (1978) 87
- [13] S. Groote, J.G. Körner and A.A. Pivovarov, *Phys. Lett.* **B443** (1998) 269
- [14] S. Groote, J.G. Körner and A.A. Pivovarov, *Nucl. Phys.* **B542** (1999) 515
- [15] S. Groote, J.G. Körner and A.A. Pivovarov, *Eur. Phys. J.* **C11** (1999) 279
- [16] S. Groote and A.A. Pivovarov, *Nucl. Phys.* **B580** (2000) 459
- [17] E. Mendels, *J. Math. Phys.* **43** (2002) 3011
- [18] A. Bashir, R. Delbourgo and M.L. Roberts, *J. Math. Phys.* **42** (2001) 5553
- [19] R. Delbourgo and M.L. Roberts, *J. Phys.* **A36** (2003) 1719
- [20] M. Caffo, H. Czyż and E. Remiddi, “Numerical evaluation of master integrals from differential equations”, [arXiv:hep-ph/0211178]
- [21] M. Caffo, H. Czyż and E. Remiddi, *Nucl. Phys.* **B634** (2002) 309
- [22] N.E. Ligterink, *Phys. Rev.* **D61** (2000) 105010;
B. Kastening and H. Kleinert, *Phys. Lett.* **A269** (2000) 50
- [23] J. Fleischer and M.Y. Kalmykov, *Phys. Lett.* **B470** (1999) 168
- [24] D.J. Broadhurst, *Z. Phys.* **C54** (1992) 599
- [25] S. Groote, J. G. Körner and A. A. Pivovarov, *Phys. Rev.* **D60** (1999) 061701
- [26] S. Laporta, *Int. J. Mod. Phys.* **A15** (2000) 5087
- [27] G. Passarino, *Nucl. Phys.* **B619** (2001) 257
- [28] A.T. Suzuki and A.G. Schmidt, *J. Comput. Phys.* **168** (2001) 207
- [29] E. Witten, *Nucl. Phys.* **B160** (1979) 57
- [30] A.I. Davydychev and M.Y. Kalmykov, *Nucl. Phys.* **B605** (2001) 266

- [31] K.G. Chetyrkin, J.H. Kühn and A. Kwiatkowski, Phys. Rep. **277** (1996) 189
- [32] S. Groote, J.G. Körner and A.A. Pivovarov, Phys. Rev. **D61** (2000) 071501;
B.L. Ioffe, Nucl. Phys. **B188** (1981) 317; **B191** (1981) 591(E)
- [33] A.A. Pivovarov and L.R. Surguladze, Nucl. Phys. **B360** (1991) 97, Yad. Fiz. **48**
(1988) 1856 [Sov. J. Nucl. Phys. **48** (1989) 1117]
- [34] A.A. Ovchinnikov, A.A. Pivovarov and L.R. Surguladze, Int. J. Mod. Phys. **A6**
(1991) 2025, Sov. J. Nucl. Phys. **48** (1988) 358 [Yad. Fiz. **48** (1988) 562]
- [35] S. Groote, J.G. Körner and A.A. Pivovarov, “Analytical calculation of heavy baryon
correlators in NLO of perturbative QCD”, [arXiv:hep-ph/0009218]
- [36] A.G. Grozin and O.I. Yakovlev, Phys. Lett. **B285** (1992) 254
- [37] R.J. Furnstahl, X.m. Jin and D.B. Leinweber, Phys. Lett. **B387** (1996) 253
- [38] X.m. Jin and J. Tang, Phys. Rev. **D56** (1997) 515
- [39] N.V. Krasnikov, A.A. Pivovarov and A.N. Tavkhelidze, Z. Phys. **C19** (1983) 301;
JETP Lett. **36** (1982) 333 [Pisma Zh. Eksp. Teor. Fiz. **36** (1982) 272]
- [40] S. Groote and A.A. Pivovarov, Eur. Phys. J. **C21** (2001) 133;
JETP Lett. **75** (2002) 221 [Pisma Zh. Eksp. Teor. Fiz. **75** (2002) 267]
- [41] A.L. Kataev, N.V. Krasnikov and A.A. Pivovarov,
Nucl. Phys. **B198** (1982) 508; **B490** (1997) 505(E) Phys. Lett. **B107** (1981) 115
- [42] A.A. Pivovarov, Phys. Atom. Nucl. **63** (2000) 1646 [Yad. Fiz. **63N9** (2000) 1734]
- [43] D.I. Kazakov, Phys. Lett. **B133** (1983) 406
- [44] D.Y. Bardin, M.S. Bilenky, D. Lehner, A. Olchevski and T. Riemann,
Nucl. Phys. Proc. Suppl. **37B** (1994) 148
- [45] I. Wetzorke and F. Karsch, “The H dibaryon on the lattice”, [arXiv:hep-lat/0208029]

- [46] S. Narison and A.A. Pivovarov, Phys. Lett. **B327** (1994) 341
- [47] S. Weinberg, Physica **A96** (1979) 327
- [48] S.A. Larin, V.A. Matveev, A.A. Ovchinnikov and A.A. Pivovarov,
Yad. Fiz. **44** (1986) 1066 [Sov. J. Nucl. Phys. **44** (1986) 690];
I.I. Balitsky, D.I. D’Yakonov and A.V. Yung, Phys. Lett. **B112** (1982) 71
- [49] T. Sakai, K. Shimizu and K. Yazaki, Prog. Theor. Phys. Suppl. **137** (2000) 121
- [50] S.R. Coleman and E. Weinberg, Phys. Rev. **D7** (1973) 1888;
R. Jackiw, Phys. Rev. **D9** (1974) 1686;
J.M. Chung and B.K. Chung, J. Korean Phys. Soc. **39** (2001) 971;
Phys. Rev. **D59** (1999) 105014
- [51] R. Jackiw and S. Templeton, Phys. Rev. **D23** (1981) 2291
- [52] K. Kajantie, M. Laine, K. Rummukainen and Y. Schröder, JHEP **0304** (2003) 036
- [53] T. Hatsuda, Nucl. Phys. **A544** (1992) 27;
T. Appelquist and R.D. Pisarski, Phys. Rev. **D23** (1981) 2305
- [54] D.J. Gross, R.D. Pisarski and L.G. Yaffe, Rev. Mod. Phys. **53** (1981) 43
- [55] T. Nishikawa, O. Morimatsu and Y. Hidaka,
“On the thermal sunset diagram for scalar field theories”, arXiv:hep-ph/0302098
- [56] J.O. Andersen, E. Braaten and M. Strickland, Phys. Rev. **D62** (2000) 045004
- [57] J.F. Yang, J. Zhou and C. Wu, “Numerical evaluation of a two loop diagram in the cut off regularization”, [arXiv:hep-ph/0301205]; H. Van Hees and J. Knoll, Phys. Rev. **D65** (2002) 105005; N.P. Mehta, C. Feline, J.R. Shepard and J. Piekarewicz, “Low-energy operators in effective theories”, [arXiv:nucl-th/0305007]
- [58] L. Platter, H.W. Hammer and U.G. Meißner, Nucl. Phys. **A714** (2003) 250

- [59] G.N. Watson, “Theory of Bessel functions”, Cambridge, 1944
- [60] K.G. Chetyrkin, A.L. Kataev and F.V. Tkachov, Nucl. Phys. **B174** (1980) 345
- [61] A.E. Terrano, Phys. Lett. **B93** (1980) 424
- [62] N.N. Bogoliubov and D.V. Shirkov, “Quantum fields”, Benjamin, 1983
- [63] A.A. Pivovarov, Phys. Lett. **B236** (1990) 214; Phys. Lett. **B263** (1991) 282
- [64] A.P. Prudnikov, Yu.A. Brychkov and O.I. Marichev,
“Integrals and Series”, Vol. 2, Gordon and Breach, New York, 1990
- [65] I.S. Gradshteyn and I.M. Ryzhik,
“Tables of integrals, series, and products”, Academic Press, 1994
- [66] Hoang Son Do, Ph. D. thesis, 2003
- [67] D.J. Broadhurst, Eur. Phys. J. **C8** (1999) 311
- [68] A.A. Pivovarov, N.N. Tavkhelidze and V.F. Tokarev, Phys. Lett. **B132** (1983) 402
- [69] K.G. Chetyrkin and A.A. Pivovarov, Nuovo Cim. **A100** (1988) 899
- [70] A.A. Pivovarov and V.F. Tokarev, Yad. Fiz. **41** (1985) 524
- [71] C.S. Meijer, Proc. Amsterdam Akad. Wet. (1940) 599; 702
- [72] A. Erdelyi (Ed.), “Tables of integral transformations”,
Volume 2, Bateman manuscript project, 1954
- [73] M. Abramowitz, I.A. Stegun (eds.), “Handbook of Mathematical Functions”,
Dover Publ. Inc., New York, 9th Printing, 1970